

## Electronic noise due to temperature difference demonstrated in molecular junctions: beyond standard thermal and shot noises

**Authors:** O. Shein Lumbroso<sup>1</sup>, L. Simine<sup>2</sup>, A. Nitzan<sup>3,4</sup>, D. Segal<sup>2</sup>, and O. Ta<sup>1</sup>

### Affiliations:

<sup>1</sup>Department of Chemical Physics, Weizmann Institute of Science, Rehovot, Israel

<sup>2</sup>Department of Chemistry, University of Toronto, Toronto, Ontario, Canada

<sup>3</sup>Department of Chemistry, University of Pennsylvania, Philadelphia, Pennsylvania, USA

<sup>4</sup>School of Chemistry, Tel Aviv University, Tel Aviv, Israel

Since the discovery of electronic thermal and shot noise a century ago<sup>1-3</sup>, these two forms of fundamental noise have an enormous impact on science and technology. They are regarded as valuable probes for quantum and thermodynamic quantities<sup>4-11</sup>, but also as an undesired noise in electronic devices that should be minimized. Electronic thermal noise is activated in equilibrium by finite temperature, whereas electronic shot noise is a non-equilibrium current noise activated by voltage<sup>8,12</sup>. Here, we report on measurements of a fundamental electronic noise that is activated by temperature difference across nanoscale conductors, which we denote as  $\Delta T$  noise (delta T noise). This noise is experimentally demonstrated in molecular junctions, and analyzed theoretically using the Landauer formalism for quantum conductors<sup>8,13</sup>. Our findings show that  $\Delta T$  noise is distinguished from the standard thermal and shot noises<sup>8</sup>. Similarly to thermal noise, it has a pure thermal origin, yet it is generated only out of equilibrium.  $\Delta T$  noise is also different from the standard electronic shot noise, since it is not created by constant<sup>8</sup> or time-dependent<sup>12,14</sup> voltage, which is applied externally or built by thermopower<sup>15</sup>.  $\Delta T$  noise can be used to detect temperature differences across nanoscale conductors without the need for fabricating sophisticated local probes. Thus, it can greatly facilitate the study of heat transport at the nanoscale. In the context of modern electronics, temperature differences are often created unintentionally across electronic components. Taking into account the contribution of the overlooked  $\Delta T$  noise in these cases, is of central importance for the design of high performance electronics at the nanometer scale.

At a finite temperature, the thermal motion of electrons leads to temporal current fluctuations called thermal

(Johnson–Nyquist) noise  $S_{TN}$ , even at zero net current in equilibrium conditions<sup>2,3</sup>. This noise depends solely on the conductance  $G$  ( $G = 1/R$ , where  $R$  is resistance), and temperature  $T$  in a straightforward manner:  $S_{TN} = 4Gk_B T$ , where  $k_B$  is the Boltzmann's factor<sup>8</sup>. Thermal noise can be used as a primarily thermometer, since it does not depend on the conductor's shape, material type, or the details of the transport mechanism<sup>4,16</sup>. Once a finite voltage is applied across a conductor and current is generated, electrons can either be transmitted through the conductor or backscatter, leading to non-equilibrium temporal current fluctuations called electronic shot noise. This noise was extensively used in the study of electronic transport in quantum conductors, including the analysis of quasiparticles' charge, electronic spin transport, and interacting many-body systems<sup>5,6,9,10</sup>. Shot noise measurements also provides unique information about electronic transport at the miniaturization limit for electronic conductors, namely across atomic and molecular junctions<sup>7,17-22</sup>. These junctions are composed from individual atoms or molecules suspended between two electrodes. The conductance of such quantum conductors is described by the Landauer formalism as the sum of contributions from several transmission channels<sup>8</sup>:  $G = G_0 \sum_i \tau_i$ . Here,  $\tau_i$  is the transmission probability of the  $i^{th}$  channel that can have any value between zero (closed channel) to one (fully open channel) and  $G_0$  is the quantum of conductance ( $G_0 \cong (12.9k\Omega)^{-1}$ ). In this framework, the current noise in quantum conductors, including both thermal and shot noises, can be described as<sup>7,8</sup>

$$S_I = 4G_0 \sum_i \tau_i^2 k_B T + 2eV \coth\left(\frac{V}{2k_B T}\right) G_0 \sum_i \tau_i (1 - \tau_i) \quad (1)$$

where  $e$  and  $V$  are the electron charge and applied voltage across the conductor, respectively. At zero applied voltage, shot noise is nullified and equation (1) is reduced to the thermal noise.

When a temperature difference  $\Delta T$ , instead of a voltage, is applied across the conductor, a new expression for the current noise can be derived based on Landauer formalism:

$$S_I = 4G_0 \sum_i \tau_i k_B \bar{T} + \left[ \frac{k_B(\Delta T^2)}{\bar{T}} \left( \frac{\pi^2}{9} - \frac{2}{3} \right) \right] G_0 \sum_i \tau_i (1 - \tau_i) \quad (2)$$

where  $\bar{T}$  is the average of  $T^h$  and  $T^c$ , the temperatures at the hot and cold sides of the conductor (Fig. 1a), and  $\Delta T = T^h - T^c$ . An expression for noise generated by temperature difference was previously derived for diffusive

conductors<sup>23</sup>. The full derivation of equation (2), including more general expressions, appears in the Supplementary Information. The first term of equation (2) is simply the thermal noise. However, when a temperature difference is applied, this term depends on the average temperature across the conductor. Remarkably, a new noise contribution (second term), which we denote as  $\Delta T$  noise, is activated as a result of temperature difference across the conductor. In contrast to standard shot noise,  $\Delta T$  noise has a pure thermal origin. Yet, similarly to shot noise, it depends on  $\sum_i \tau_i(1 - \tau_i)$  despite the absence of voltage gradient across the conductor. Such dependence on the transmission probabilities is the signature of partition noise<sup>8</sup>. Namely, noise that is activated in non-equilibrium conditions by the partial transmission and backscattering of transporting electrons. For  $\Delta T$  noise, non-equilibrium conditions are introduced by temperature difference and partition noise is activated even in the ideal case of zero net current due to opposite and equal currents above and below the chemical potential (Fig. 1b). Thus,  $\Delta T$  noise can be viewed as partition noise that is generated by temperature difference.

To experimentally demonstrate the effect of temperature difference on the noise generated in a quantum conductor, we studied molecular junctions based on hydrogen molecules introduced between two atomically sharp gold electrodes<sup>24,25</sup>. We use the break junction technique<sup>26</sup> (Fig. 1a and Methods) to form an ensemble of molecular junctions with different local structure and hence different conductance (Extended Data Fig. 1). Shot noise measurements indicate that below  $1 G_0$  the conductance of the junction is usually governed by a dominant transmission channel (see Methods and Extended Data Fig. 4). Its transmission probability can be varied, for example, by adjusting the separation between the electrodes in sub-angstrom resolution<sup>26</sup>. In the actual experiment, some secondary transmission channels may also contribute to the total conductance. A temperature gradient across the junction was applied by asymmetric heating of the junction's electrodes above a base temperature of 4.2 K. The temperature difference across the junction was monitored by two thermometers located at the opposite sides of the junction (Fig. 1a). In order to determine the temperature at the nanoscale

vicinity of the junction, the thermometers were calibrated using the thermal noise generated in the junction, when no temperature difference was applied (see Methods).

To test the validity of the first term of equation (2), a temperature gradient should be applied, while the second term (the  $\Delta T$  noise) should be suppressed. Practically, these conditions can be met in two ways. When the conductance of the studied junction is dominated by a single channel with transmission probability close to one

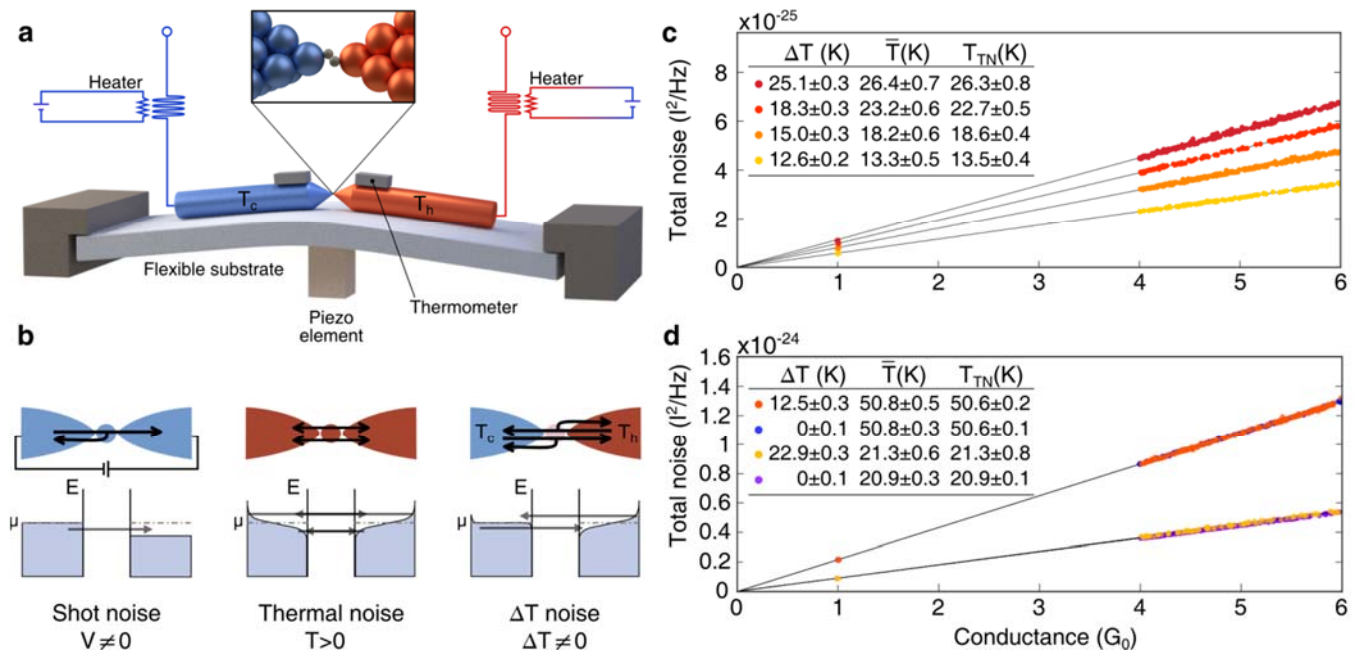


**Figure 1. Experimental setup, different noise contributions, and measured thermal noise at a finite temperature difference.** **a**, Schematic illustration of the break junction setup, including heaters and thermometers. **Inset**, schematic illustration of the Au\H<sub>2</sub> junction. **b**, Schematic illustration of the standard shot noise, thermal noise and  $\Delta T$  noise in an atomic-scale junction. **c**, Total noise as a function of conductance measured in the studied atomic scale junctions at different temperatures  $T_{th}^h$  and  $T_{th}^c$  at the opposite sides of the junctions. At  $1G_0$  and above  $4G_0$  the total noise is dominated by thermal noise (first term in equation (2)). In these conditions, a linear dependence of the noise on the conductance is expected. **Inset tables**, present the temperature difference  $\Delta T$  and average temperature  $\bar{T}$  measured by the thermometers at the opposite junction's sides, as well as the temperature extracted from the slop of the thermal noise  $T_{TN}$ . For a given conductance, the thermal noise is exclusively determined by the average temperature of the hot and cold electrodes. **d**, Four sets of total noise data as in (c). Each couple of data sets is taken at similar  $\bar{T}$ , yet one set is measured at  $\Delta T \neq 0$  and another at  $\Delta T = 0$ . The presented data illustrate that similar thermal noise is generated at different  $\Delta T$  as long as  $\bar{T}$  is similar. The data error bars are smaller than the symbols' diameter, and the calculations of the  $\Delta T$  and  $\bar{T}$  errors presented in the inset tables take into consideration the incomplete suppression of noise contributions beyond the thermal noise.

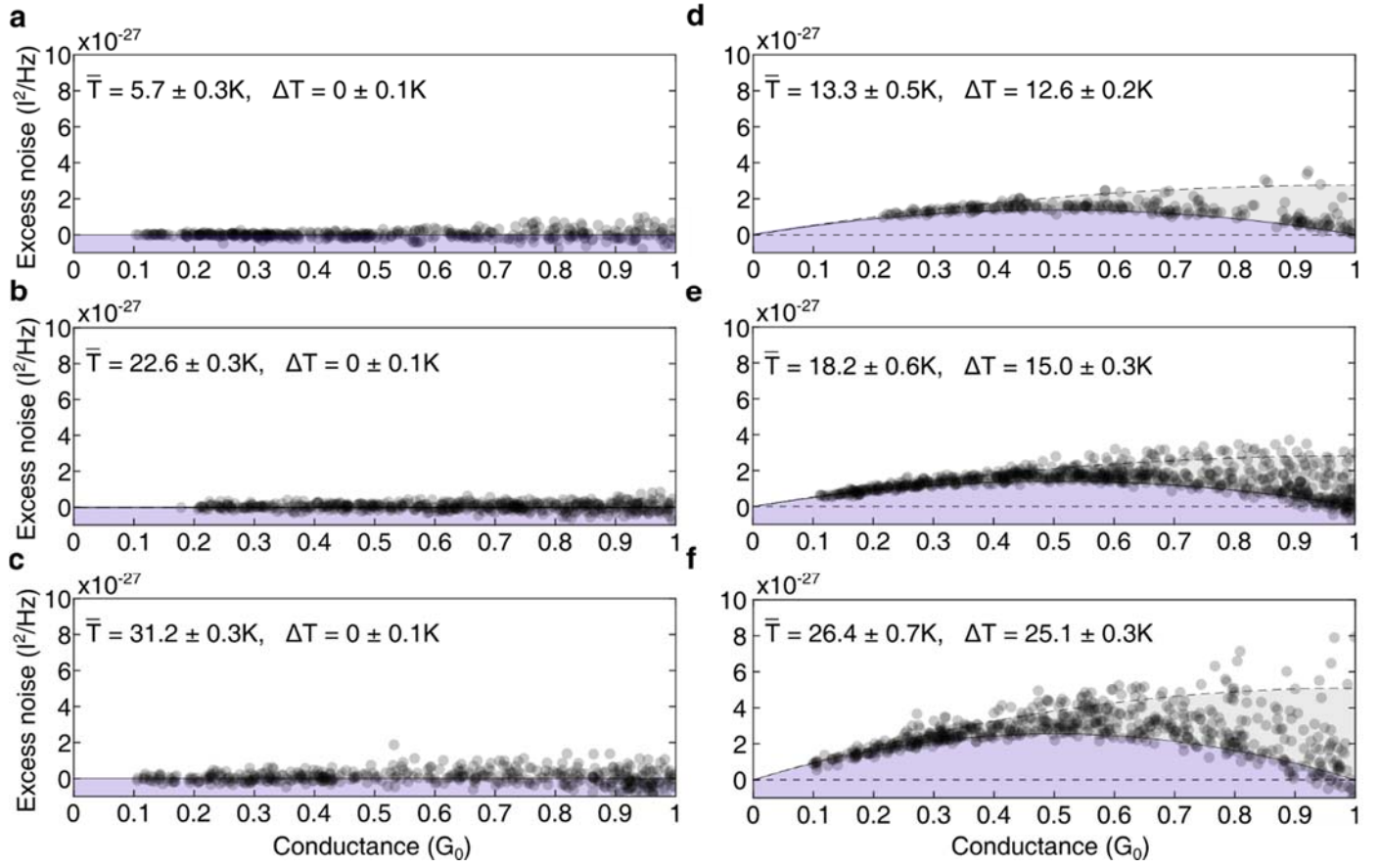
$(\tau \geq 1)$ , the second term is expected to be very small. These conditions are indeed achieved in some junction realizations, as indicated by shot noise measurements (Extended Data Fig. 4). Furthermore, the relative contribution of the second term with respect to the first one depends on  $(\Delta T/\bar{T})^2$  and the Fano factor  $F = \sum_i \tau_i (1 - \tau_i) / \sum_i \tau_i$ . The Fano factor can be determined by shot noise measurements on similar junctions. We found that if the junction is squeezed to form a multi-atomic gold contact<sup>7</sup> with conductance higher than  $4 G_0$ , the maximal contribution of the second term in equation (2) is less than 5% with respect to the first term in the examined conditions, and typically around 3% (see Methods and Extended Data Fig. 4).

Figure 1c shows the measured total noise as a function of conductance for the studied junctions at different average junction temperature and temperature difference (see Methods), determined by the calibrated thermometers at the hot and cold sides of the junction. We attribute the linear dependence on the conductance to efficient suppression of the second term in equation (2) at  $1 G_0$  and above  $4 G_0$ . In these conditions, the total noise is practically reduced to the thermal noise, and the temperature associated with the thermal noise  $T_{TN}$ , can be extracted from the slope of each curve. The inset table in Fig. 1c shows that  $T_{TN} = \bar{T}$  in the error range, indicating that the thermal noise generated at the junction depends on the average temperature of the junction. Fig. 1d presents two examples for total noise vs. conductance measured at comparable average temperature of about  $\bar{T} = 21 K$ , as well as  $\bar{T} = 51 K$ . In each example, the temperature difference across the examined junction is set to be either zero ( $\Delta T = 0$ ) or finite ( $\Delta T \neq 0$ ), as seen in the inset table. The data points clearly fall on top of each other, illustrating that the thermal noise is exclusively determined by the average temperature and it does not depend on the temperature difference.

We will now focus on experimental indications for the activation of  $\Delta T$  noise and identify its properties. Figure 2 presents measurements of excess noise as a function of conductance for different temperature differences and average temperatures. A conductance range of  $0.1 < G < 1 G_0$  was chosen in order to look for the  $\tau(1 - \tau)$  dependence of the  $\Delta T$  noise. The excess noise is defined as the total noise minus the average thermal noise. The

latter is obtained as presented in Fig. 1c and explained above. The sets of measurements at  $\Delta T = 0K$  (Fig. 2a-c) simply yield data around zero excess noise. In the absence of temperature difference across the junctions the total noise is governed by the thermal noise. Thus, subtracting the average thermal noise from the total noise gives values that are scattered around zero. Remarkably, when a temperature difference is applied across the junction, a finite excess noise is activated (Fig. 2d-f), indicating that the origin of the measured noise is temperature difference. We note that even in the absence of applied voltage, shot noise alone can yield excess noise at a finite temperature difference, as a consequence of a buildup of thermoelectric voltage<sup>15</sup>. However, the expected shot noise due to thermoelectric voltage is about three orders of magnitude lower than the measured excess noise in Fig. 2d-f. This is illustrated in Extended Data, Fig. 6, by measuring the total thermoelectric voltage produced in our experiments and calculating the shot noise that can be generated by the highest thermoelectric voltage that was found (see Methods). Thus, the contribution of shot noise due to thermoelectric voltage is insignificant with respect to the measured excess noise at a finite temperature difference and cannot explain its origin.

The lower boundary of the measured excess noise in Fig. 2d-f is very well described by the calculated  $\Delta T$  noise, assuming a single transmission channel (solid curve). In fact, most of the data points accumulate in the vicinity of this curve, indicating the activation of  $\Delta T$  noise in junctions with significant conductance contribution from one transmission channel. As the conductance increases, the spread of the measured noise towards higher values increases as well. This characteristic trend is captured by the dashed line that gives the calculated  $\Delta T$  noise for junctions with two channels having similar transmission probabilities. Independent shot noise measurements (see Methods and Extended Data, Fig. 4) indicate that most of the examined molecular junctions are characterized by transport via a dominant channel, though some of the junctions can have significant conductance contribution from a second channel or (in rare cases) from additional channels. Based on these channel analysis,  $\Delta T$  noise is expected to yield excess noise data, which is mainly located in the gray area, as indeed observed. Thus, the characteristics of the measured excess noise fit the expected behavior of  $\Delta T$  noise in the examined junctions. Using equation (2), we can extract the Fano factor from the excess noise that is generated by temperature



**Figure 2. Excess noise measured at zero and finite temperature difference.** **a-c**, Excess noise (obtained by subtracting the average thermal noise from the total measured noise) as a function of conductance measured in the examined molecular junctions at different temperatures and no temperature difference across the junctions ( $\Delta T = 0$ ). **d-f**, Excess noise as a function of conductance measured at different average temperatures and finite temperature differences across the junctions ( $\Delta T \neq 0$ ). The expected  $\Delta T$  noise (based on exact numerical solution, see supplementary information, equation (S7)) is given by the black curve for a single transmission channel, and by the dashed curves for two channels with equal transmission probabilities. The error bars are slightly larger than the diameter of the symbols as shown in Extended data Fig. 7. Once that a temperature difference is applied across the junctions, a clear enhancement of the excess noise is observed. The measured excess noise can be described by the theoretical expression for the  $\Delta T$  noise, where the spread in the results is a natural outcome of additional transmission channels that are opened as the conductance increases (see Extended Data, Fig. 4).

difference. Extended Data Fig. 6 shows that the Fano factor distribution obtained in this way is similar to the one obtained by shot noise measurements (Extended Data Fig. 4), further demonstrating that the excess noise at finite temperature difference is actually the  $\Delta T$  noise given by the second term of equation (2).

The quadratic dependence of the  $\Delta T$  noise on the temperature difference is a distinctive fingerprint of this noise. To check if the detected excess noise shows the expected dependence on temperature difference, we normalized the measured excess noise, based on equation (2), and plotted it with respect to  $\Delta T$  in Fig. 3. The data speared is asymmetric and can be described by a generalized extreme value distribution (Fig. 3, Inset). The most probable normalized excess noise (red rectangles) fits well the dashed curve that describes the quadratic dependence of the  $\Delta T$  noise on the temperature difference for a single channel scenario. The upward spread of the data (transparent black circles) can be explained by the presence of junctions with more than one transmission channel, where most of the data falls below the dotted curve that shows the  $\Delta T$  noise dependence on  $(\Delta T)^2$ , assuming two channels with similar transmission probabilities. The observation of this fingerprint of  $\Delta T$  noise provides a complimentary indication that we measure the  $\Delta T$  noise given by the theoretical description.

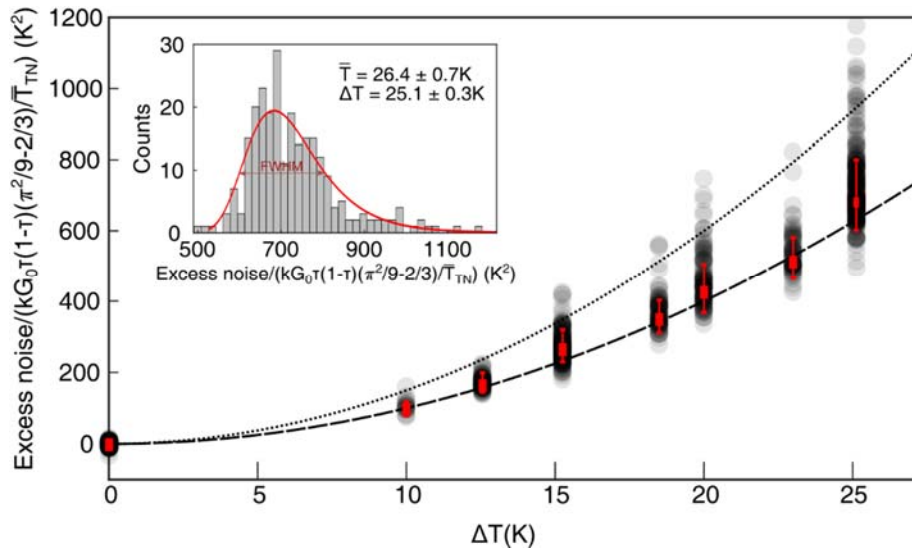


**Figure 3. Excess noise dependence on the applied temperature difference.** Normalized most-probable excess noise as a function of  $\Delta T$ . The normalization is given by equation (2), in order to test a possible  $(\Delta T)^2$  dependence expected for  $\Delta T$  noise. The solid line shows the expected normalized  $\Delta T$  noise assuming a single transmission channel. The dashed lines show the expected normalized  $\Delta T$  noise assuming two channels with equal transmission probability. The most probable excess noise shows a clear  $(\Delta T)^2$  dependence as expected for  $\Delta T$  noise. The most probable excess noise was determined by a generalized extreme value distribution that captures the asymmetric distribution of the data, and the error bars are determined by the full width at half maximum as illustrated in the inset, which describes the analysis of the data at  $\Delta T \approx 25 K$  in the main figure.

To conclude, our experimental findings supported by a theoretical derivation indicate that partition noise emerges in the presence of a temperature gradient across quantum conductors. We denote this noise contribution as the  $\Delta T$  noise and show that it possesses a peculiar combination of characteristics that makes it distinctive from the standard thermal and shot noises. Beyond the fundamental interest in the observation and characterization of a temperature-difference-based form of partition noise, the  $\Delta T$  noise can be used as a spectroscopic probe for temperature differences. This ability is particularly interesting for probing temperature differences at the nanoscale since fabricating physical probes that measure local temperature at this scale is extremely challenging. In contrast to physical sensors, the  $\Delta T$  noise is a very versatile probe, which is not limited to a specific temperature range, and can be applied to different conductors' sizes, down to the atomic scale.  $\Delta T$  noise measurements can be done without special design limitations in a variety of setups, including scanning probe microscopes, nanoscale devices, and even in embedded systems, which are not very accessible to temperature sensing. This flexibility makes the  $\Delta T$  noise an attractive tool for the study of heat management, including thermoelectricity, heat pumping, and heat dissipation, which are important in the context of energy saving and sustainable energy production. Last but not least, temperature gradients are unintentionally formed in electronic circuits. Therefore, the overlooked  $\Delta T$  noise in these cases should be taken into consideration as a limiting factor for modern nanoscale electronics.

## References:

1. Schottky, W. Über spontane Stromschwankungen in verschiedenen Elektrizitätsleitern. *Ann. Phys.* **362**, 541-567 (1918).
2. Johnson, J. B. Thermal Agitation of Electricity in Conductors. *Nature* **119**, 50-51 (1927).
3. Nyquist, H. Thermal Agitation of Electric Charge in Conductors. *Phys. Rev.* **32**, 110-113 (1928).
4. Garrison, J.B. & Lawson, A.W. An absolute noise thermometer for high temperatures and high pressures. *Rev. Sci. Instrum.* **20**, 785 (1949)
5. Saminadayar, L., Glattli, D. C., Jin Y. & Etienne, B. Observation of the  $e/3$  Fractionally Charged Laughlin Quasiparticle. *Phys. Rev. Lett.* **79**, 2526 (1997)

6. De-Picciotto, R., Reznikov, M., Heiblum, M., Umansky, V., Bunin G. & Mahalu, D. Direct observation of a fractional charge. *Nature* **389**, 162-164 (1997).
7. van den Brom, H. E. & van Ruitenbeek, J. M. Quantum suppression of shot noise in atom-size metallic contacts. *Phys. Rev. Lett.* **82**, 1526–1529 (1999).
8. Blanter, Y. M. & Büttiker, M. Shot noise in mesoscopic conductors. *Phys. Rep.* **336**, 1-66 (2000).
9. Roche, P. et al. Fano factor reduction on the 0.7 conductance structure of a ballistic one-dimensional wire. *Phys. Rev. Lett.* **93**, 116602 (2004).
10. Delattre, T. et al. Noisy Kondo impurities. *Nat. Phys.* **5**, 208-212 (2009)
11. Jezouin, S. et al. Controlling charge quantization with quantum fluctuations. *Nature* **536**, 58-62. (2016)
12. Schoelkopf, R. J., Kozhevnikov, A. A., Prober, D. E. & Rooks, M. J. Observation of ‘photon-assisted’ shot noise in a phase-coherent conductor. *Phys. Rev. Lett.* **80**, 2437 (1998).
13. Buttiker, M., Imry, Y., Landauer, R. & Pinhas, S. Generalized many-channel conductance formula with application to small rings *Phys. Rev. B* **31**, 6207 (1985).
14. Reydellet, L.-H., Roche, P., Glattli, D. C., Etienne, B. & Jin, Y. Quantum partition noise of photon-created electron-hole pairs. *Phys. Rev. Lett.* **90**, 176803 (2003).
15. Reddy, P., Jang, S.Y., Segalman, R.A. & Majumdar, A. Thermoelectricity in molecular junctions. *Science* **315**, 1568-1571 (2007).
16. White, D.R. et al. The status of Johnson noise thermometry. *Metrologia* **33**, 325-335 (1996).
17. Djukic, D. & van Ruitenbeek, J. M. Shot noise measurements on a single molecule. *Nano Lett.* **6**, 789-793 (2006).
18. Tal, O., Krieger, M., Leerink, B. & van Ruitenbeek, J. M., Electron-vibration interaction in single-molecule junctions: From contact to tunneling regimes. *Phys. Rev. Lett.* **100**, 196804 (2008).
19. Chen, R., Matt, M., Pauly, F., Cuevas, J. C. & Natelson, D. Shot noise variation within ensembles of gold atomic break junctions at room temperature. *J. Phys. Condens. Matter.* **26**, 474204 (2014).
20. Burtzlaff, A., Weismann, A., Brandbyge, M. & Berndt, R. Shot noise as a probe of spin-polarized transport through single atoms. *Phys. Rev. Lett.* **114**, 016602. (2015).
21. Vardimon, R., Klionsky, M. & Tal, O. Indication of complete spin filtering in atomic-scale nickel oxide. *Nano Lett.* **15**, 3894-3898 (2015).
22. Karimi, M. A., Bahoosh, S. G., Herz, M., Hayakawa, R., Pauly, F. & Scheer, E., Shot noise of 1, 4-benzenedithiol single-molecule junctions. *Nano Lett.* **16**, 1803-1807 (2016).
23. Sukhorukov, E.V. & Loss, D. Noise in multiterminal diffusive conductors: Universality, nonlocality, and exchange effects. *Phys. Rev. B.* **59**, 13054 (1999).

- 24.** Csonka, S., Halbritter, A. & Mihály, G. Pulling gold nanowires with a hydrogen clamp: Strong interactions of hydrogen molecules with gold nanojunctions. *Phys. Rev. B.* **73**, 075405 (2006).
- 25.** Nakazumi, T., Kaneko, S. & Kiguchi, M. Electron transport properties of Au, Ag, and Cu atomic contacts in a hydrogen environment. *J. Phys. Chem. C.* **118**, 7489-7493 (2014).
- 26.** Muller, C.J., van Ruitenbeek, J. M. & De Jongh, L. J. Experimental observation of the transition from weak link to tunnel junction. *Physica C* **191**, 485-504 (1992).